

Effects of static crystal field on the homogeneous width of the 5D_0 - 7F_0 line of Eu^{3+} and Sm^{2+} in solids

Masanori Tanaka and Takashi Kushida

Department of Physics, Osaka University, Toyonaka, Osaka 560, Japan

(Received 12 December 1994)

The rates of the phase relaxations due to the Raman scattering of phonons and the interaction of the optical center with flipping two-level systems (TLS) have been calculated for the 5D_0 - 7F_0 line of the Eu^{3+} and Sm^{2+} ions in solids, by taking into account the mixing between the $4f^6$ states (J mixing) through the static crystal-field potential. The results have been compared with the previously reported experimental data on the wavelength dependence of the homogeneous width of the inhomogeneously broadened 5D_0 - 7F_0 transition of Eu^{3+} and Sm^{2+} in several kinds of glasses at various temperatures. It has been found that the experimental data in the temperature region above about 10 K, where the homogeneous width shows nearly quadratic temperature dependence, are accounted for well, by assuming that the homogeneous width of this transition in glasses is dominated by the two-phonon Raman process in the 7F_0 state, which occurs via the $M_J=0$ component of the 7F_2 manifold mixed into 7F_0 through the axial second-order crystal-field potential. On the other hand, the above wavelength dependence observed in the Eu^{3+} -doped silicate glass at liquid-He temperature can be explained well by the calculation based on the interpretation that the difference between the permanent electric dipole moments in the 5D_0 and 7F_0 states of the rare-earth ion which interacts with TLS is caused by the J mixing. In addition, the probability of the one-phonon 7F_0 - 7F_1 absorption process has been calculated. The mixing of the 7F_2 state into 7F_0 and 7F_1 by the second-order crystal-field components is shown to play an essential role in this process.

I. INTRODUCTION

During the last two decades, a large number of studies have been made on the homogeneous spectral widths and shapes of the optical electronic transitions of paramagnetic ions and dye molecules in glassy materials from both experimental and theoretical points of view.¹ These studies are important for the clarification of the dephasing mechanism of optical centers in glasses, because information on this mechanism is obtainable from the homogeneous spectra.

Since the beginning of this field, it has been found that the homogeneous width $\Delta\nu_{\text{hom}}$ varies with energy within the inhomogeneous absorption profile of the 5D_0 - 7F_0 transition of the Eu^{3+} ion in several kinds of glasses at various temperatures.²⁻⁶ It has been pointed out that the Eu^{3+} ion in the stronger crystal field has the larger homogeneous width. Furthermore, Morgan's group⁴ explained the above phenomenon, assuming that $\Delta\nu_{\text{hom}}$ is proportional to the square of the coupling coefficient between the Eu^{3+} ion and the two-level systems (TLS) and that the coupling strength is stronger at the Eu^{3+} site with a stronger crystal field. However, their explanation was fairly qualitative.

Several theories^{5,7,8} have shown that the nearly quadratic temperature dependence of $\Delta\nu_{\text{hom}}$ observed for the 5D_0 - 7F_0 transition in various Eu^{3+} -doped glasses in a very wide temperature range above about 10 K (Refs. 3,5,9-11) can be explained by the relaxation due to the two-phonon Raman process. On the other hand, the linear temperature dependence of $\Delta\nu_{\text{hom}}$ has been ob-

served for the same transition of Eu^{3+} in silicate glasses between 0.4 and 4.2 K by transient hole burning^{6,12} and between 1.6 and 7 K by photon echoes.¹¹ This temperature dependence is consistent with the dependence derived by several authors^{9,13-15} on the basis of the interaction of the optically active center with the TLS. Yano and co-workers¹¹ have recently shown that contributions from both the two-phonon Raman process and the interaction between the Eu^{3+} ion and the TLS are important in explaining the quadratic temperature dependence observed between 10 and 40 K for the 5D_0 - 7F_0 transition of the Eu^{3+} ion in a pure silicate glass fiber.

In this paper, we report a detailed analysis of the energy dependence of $\Delta\nu_{\text{hom}}$ in the 5D_0 - 7F_0 transition of the Eu^{3+} and Sm^{2+} ions in glasses. Recently, it has been proved by our group^{16,17} that J mixing, i.e., the mixing between the $4f^6$ states through the static crystal-field potential, contributes dominantly to the fluorescence intensity and the inhomogeneous broadening of the 5D_0 - 7F_0 transition of the Eu^{3+} ion in oxide glasses. In Sec. II, we calculate the probabilities of the phase relaxation due to the Raman process of phonons in the 7F_0 and 5D_0 states, and the homogeneous width of the 5D_0 - 7F_0 transition due to the electric dipole-dipole interaction between the Eu^{3+} ion and the TLS, by taking into account the J -mixing effect. The results account well for the energy dependence of $\Delta\nu_{\text{hom}}$ of the 5D_0 - 7F_0 transition in glasses. Furthermore, in Sec. III, we discuss the effect of the static crystal field on the one-phonon 7F_0 - 7F_1 absorption process, which has been shown to determine the homogeneous width of the same transition of Eu^{3+} in YAlO_3 crys-

tals.⁹ Up to now, many researchers have investigated the homogeneous width (or the hole width in the hole-burning experiment) or the optical dephasing rate of the f - f transition of rare-earth-doped materials.^{1-15,18-37} To our knowledge, however, this is the first study to investigate the contribution of J mixing to the dephasing relaxation in that sort of transition.

The Sm^{2+} ion has the same $4f^6$ electron configuration as Eu^{3+} , and the structure of the low-energy electronic energy levels and their wave functions are almost the same between these ions.³⁸ Therefore, most of the analyses made for the Eu^{3+} ion are also applicable to the case of Sm^{2+} .

The 5D_0 - 7F_0 line of Eu^{3+} and the isoelectronic Sm^{2+} in the crystalline and glassy materials is simple without degeneracy and usually shows much narrower homogeneous width compared with the inhomogeneous one, especially at low temperatures. Therefore, much interest has been focused on this line of Eu^{3+} - and Sm^{2+} -doped materials from the viewpoint of practical applications to wavelength-selective optical memory devices.^{22,25,26,29-34} Our results provide useful information for the development of materials for these applications.

II. ANALYSIS OF THE WAVELENGTH DEPENDENCE OF THE HOMOGENEOUS WIDTH OF THE 5D_0 - 7F_0 TRANSITION IN GLASSES

A. Dephasing due to the two-phonon Raman process

In this section, we calculate the probabilities of the two-phonon Raman scattering in the 7F_0 and 5D_0 states of the Eu^{3+} and Sm^{2+} ions. Let us express the interaction of the rare-earth ion with the host lattice in terms of a power series of the dynamical strain ε due to the lattice vibration as follows:

$$V = V^{(0)} + V^{(1)}\varepsilon + V^{(2)}\varepsilon^2 + \dots \quad (1)$$

Here, $V^{(n)}$ is the n th-order expansion coefficient of V with respect to ε . We have used the long-wavelength approximation for phonons and assumed that $V^{(n)}$ ($n \geq 1$) are independent of the modes of phonons. In this expression, $V^{(0)}$ represents the static crystal-field potential, and it does not contribute to the phonon-induced relaxation directly. The one-phonon absorption and emission (direct processes) arise from the first-order perturbation due to the second term, while the Raman process occurs due to the $V^{(1)}\varepsilon$ term in second order and also due to the $V^{(2)}\varepsilon^2$ term in first order. Thus the probabilities of the two-phonon Raman process in the 7F_0 and 5D_0 states include the following two types of matrix elements of $V^{(1)}$ and $V^{(2)}$.^{39,40}

$$\langle A \rangle = \langle 4f^{6,2S+1}L_0 | V^{(2)} | 4f^{6,2S+1}L_0 \rangle \quad (2)$$

and

$$\langle B \rangle = \sum_{m \neq 2S+1L_0} \frac{|\langle 4f^{6,2S+1}L_0 | V^{(1)} | m \rangle|^2}{E(2S+1L_0) - E(m) \pm w_p} \quad (3)$$

Here (S, L) is $(2, D)$ for 5D_0 and $(3, F)$ for 7F_0 , and $E(m)$

and w_p are the energy of the electronic state m of the Eu^{3+} or Sm^{2+} ion in solids and the phonon energy, respectively. Since the energy separation between the $4f^6$ states is not so small compared with the phonon energy, we have neglected the case that the initial and final states of the two-phonon Raman transition are different. We expand $V^{(0)}$ and $V^{(n)}$ ($n \geq 1$) as^{40,41}

$$V^{(0)} = \sum_k V_k^{(0)} = \sum_{k,q} \sum_i B_{kq} C_{kq}(\theta_i, \phi_i) \quad (4)$$

and

$$V^{(n)} = \sum_{k,q} \sum_i V_{kq}^{(n)} C_{kq}(\theta_i, \phi_i), \quad (5)$$

with

$$C_{kq}(\theta_i, \phi_i) = \sqrt{\frac{4\pi}{2k+1}} Y_{kq}(\theta_i, \phi_i),$$

where $Y_{kq}(\theta_i, \phi_i)$ is the q component of the k th-order spherical harmonics, (r_i, θ_i, ϕ_i) is the position of the i th $4f$ electron of the rare-earth ion, and B_{kq} is the k th-order crystal-field parameter.

We first adopt the wave functions without the J mixing for the 7F_0 and 5D_0 states. Then the matrix element $\langle A \rangle$ vanishes. We consider only the $4f^6$ configuration states as the intermediate state m of the expression (3), because the states of the other electron configurations are far from the 7F_0 and 5D_0 states in energy. In this case, $\langle B \rangle$ is nonzero for the intermediate state m with even J . Among all the phonon Raman processes in the 7F_0 and 5D_0 states, the probability of the Raman scattering in the 7F_0 state through the intermediate state of 7F_2 is considered to be largest for the following two reasons. The first is that the absolute value of the matrix element $\langle 4f^6[{}^7F]_0 | C_{2q} | 4f^6[{}^7F]_2 \rangle$ is larger than those of $\langle 4f^6[{}^7F]_0 | C_{kq} | 4f^6[{}^7F]_J \rangle$ ($J = k = 4, 6$) and $\langle 4f^6[{}^5D]_0 | C_{kq} | 4f^6[{}^5D]_J \rangle$ ($J = k = 2, 4$). Here $[\dots]$ denotes that the quantities in the square brackets are not good quantum numbers because of the mixing within the $4f^6$ electron configuration states through the spin-orbit interaction. The second is that the 7F_2 - 7F_0 energy separation is smaller than the 7F_4 - 7F_0 , 7F_6 - 7F_0 , and 5D_J ($J = 2, 4$)- 5D_0 separations. (See Fig. 1 for the energy levels due to the $4f^6$ electron configuration of the Eu^{3+} and Sm^{2+} ions.) Thus we consider only the contribution from the Raman process in the 7F_0 state through the intermediate state 7F_2 . In the following, we make calculations by regarding the 7F_J states in a free-ion state as pure Russell-Saunders states, because, according to Ofelt,³⁸ the L - S coupling holds fairly well for the 7F_J states of the Eu^{3+} and Sm^{2+} ions. Then, in the case of $2S+1L_J = {}^7F_0$ and $m = {}^7F_2$, $\langle B \rangle$ is calculated as

$$\langle B \rangle = \frac{4}{75\{E({}^7F_0) - E({}^7F_2)\}} \sum_{q=-2}^2 |V_{2q}^{(1)}|^2. \quad (6)$$

Here we have neglected the mixing within the 7F_2 manifold by the static crystal-field potential and also the energies w_p of the phonons which contribute to the homo-

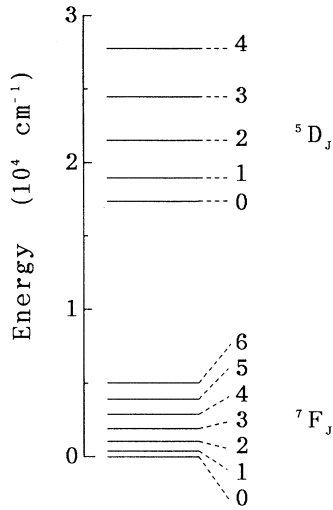


FIG. 1. Diagram of the energy levels due to the $4f^6$ electron configuration of the Eu^{3+} ion. The 5L_J and 5G_J multiplets, which lie between the 5D_3 and 5D_4 states, are omitted in this diagram. The structure of the electronic energy levels of Sm^{2+} is the same as this diagram, although the energy separations between the levels of Sm^{2+} are smaller than those of Eu^{3+} . The numbers in the diagram represent the inner quantum numbers J of the 7F_J and 5D_J multiplets.

geneous width of the 5D_0 - 7F_0 transition in expression (3) under the assumption that they are much smaller than the 7F_2 - 7F_0 energy separation, $E({}^7F_2)$ - $E({}^7F_0)$ ($\sim 1000 \text{ cm}^{-1}$).

Next, we take into account the J -mixing effect in the calculation. Although $J=2,4,6$ states admix into the $J=0$ state by the even-parity components of the crystal-field potential, we neglect the J mixing for the 5D_0 state and consider only the mixing of the 7F_2 state into 7F_0 for the same reasons that we mentioned above. Then the wave function and the energy of the 7F_0 state are written, by the perturbation calculation, respectively, as

$$|4f^6[{}^7F_0]\rangle = |4f^6[{}^7F_0]_0\rangle - \frac{2\sqrt{3}}{15\Delta_{20}} \sum_{q=-2}^2 (-1)^q B_{2q} |4f^6[{}^7F_2]_{M_J=q}\rangle. \quad (7)$$

and

$$E(4f^6[{}^7F_0]) = E_0({}^7F_0) - \frac{4}{75\Delta_{20}} \sum_{q=-2}^2 |B_{2q}|^2, \quad (8)$$

where $E_0({}^{2S+1}L_J)$ and $\Delta_{JJ'}$ are the energy of the ${}^{2S+1}L_J$ state at a free-ion state and the energy separation between the 7F_J and ${}^7F_{J'}$ states, respectively, and M_J is the inner magnetic quantum number. The matrix element $\langle A \rangle$ for $(S,L)=(3,F)$ is calculated, using the wave function of Eq. (7), as

$$\langle A \rangle = -\frac{8}{75\Delta_{20}} \sum_{q=-2}^2 (B_{2q} V_{2-q}^{(2)}). \quad (9)$$

Here we have neglected the higher-order terms of the second-order crystal-field parameters. We may put $B_{2\pm 1}=0$ in expressions (7) and (8), because the point symmetry of the Eu^{3+} or Sm^{2+} ion site in glasses under consideration is C_s , C_2 , or C_{2v} .^{16,17,42,43} Thus, the probability of the Raman scattering of phonons in the 7F_0 state is obtained, using Eqs. (6) and (9), as

$$W_R = \frac{256\pi^2}{5625h\Delta_{20}^2} \int \left| V_{20}^{(2)} B_{20} X + (B_{22} V_{2-2}^{(2)} + B_{2-2} V_{22}^{(2)}) X + \left[\sum_{q=-2}^2 |V_{2q}^{(1)}|^2 \right] Y \right|^2 D(\omega_p)^2 d\omega_p, \quad (10)$$

with

$$X = \langle n_\lambda - 1, n_\mu + 1 | \varepsilon^2 | n_\lambda, n_\mu \rangle \quad (11)$$

and

$$Y = \langle n_\lambda - 1 | \varepsilon | n_\lambda \rangle \langle n_\mu + 1 | \varepsilon | n_\mu \rangle. \quad (12)$$

Here $D(\omega_p)$ is the density of states of phonons. Furthermore, h and n_a ($a = \lambda, \mu$) are the Planck constant and the occupation number of the phonon of mode a , which has the energy ω_p , respectively. In expression (10), we have assumed that the energy separation between the 7F_2 and 7F_0 manifolds in solids, $E({}^7F_2)$ - $E({}^7F_0)$, in expression (6) is equal to that at a free-ion state, Δ_{20} . On the other hand, the probability of the two-phonon Raman scattering in the 5D_0 state is much smaller than that in the 7F_0 state, as is obvious from the above discussions. Accordingly, the homogeneous width of the 5D_0 - 7F_0 transition of Eu^{3+} and Sm^{2+} in glasses is considered to be determined by Eq. (10).

Morgan and his co-workers⁴ found that the homogeneous width within the inhomogeneous profile of the 5D_0 - 7F_0 transition of the Eu^{3+} ion in various oxide glasses is linearly correlated with the transition energy at room temperature. This transition energy is expressed as

$$E({}^5D_0\text{-}{}^7F_0) = E_0({}^5D_0) - E_0({}^7F_0) + \frac{4}{75\Delta_{20}} (B_{20}^2 + 2|B_{22}|^2), \quad (13)$$

where $E_0({}^5D_0)$ and $E_0({}^7F_0)$ are the energies of the 5D_0 and 7F_0 states in a free-ion state, respectively. In this expression, the energy of the 5D_0 state has been approximated by the free-ion energy, because it is theoretically predicted to be insensitive to the crystal-field perturbation for the same reasons that were mentioned above. Further, $|B_{22}|$ is almost constant for various Eu^{3+} ion sites in oxide glasses.^{16,17,42} Therefore, the site dependence of the 5D_0 - 7F_0 energy separation is determined mainly by the axial second-order crystal-field parameter B_{20} . As far as the wavelengths of the phonons that contribute effectively to expression (10) are much longer than the separations between the Eu^{3+} ion and the surrounding oxygens, we may consider that the density of states of such phonons is almost independent of the magnitude of the crystal field acting on the Eu^{3+} ion in oxide glasses. Then the above experimental result is explained well by

Eq. (10), provided that the absolute value of the first term in $|\cdots|$ of this equation is large enough compared with those of the other terms and that the variation of $V_{20}^{(2)}$ with the Eu^{3+} ion site is negligible. In short, the experimental data are interpreted as follows: The homogeneous width of the 5D_0 - 7F_0 line in oxide glasses is dominated, at high temperatures, by the two-phonon Raman process which occurs via the 7F_2 component mixed into the 7F_0 state through the axial second-order crystal-field potential. Furthermore, the 7F_0 state is pushed downward by the crystal-field mixing of 7F_2 . Since both of the two-phonon Raman rate and the energy shift of the 7F_0 state are proportional to B_{20}^2 , there exists a linear relation between $\Delta\nu_{\text{hom}}$ and the 7F_0 - 5D_0 transition energy. In the case of Eu^{3+} in calcium metaphosphate glass, some deviation from the linear relation has been observed.² This can also be explained by Eq. (10) by considering that the second and third terms in $|\cdots|$ are not negligible.

In the above discussion, we have neglected the J -mixing effect for $\langle B \rangle$. This approximation is considered to be good, because the contribution of the J mixing to the expression (3) is small compared with $\langle B \rangle$ of Eq. (6). We have not considered the crystal-field-induced mixing within the 7F_2 manifold in deriving Eq. (6). When the point symmetry of the Eu^{3+} ion site is sufficiently low, such as in the case of glassy host, this mixing is caused by the second- and fourth-order components of the static crystal-field potential. Thus the third term of $|\cdots|$ in Eq. (10) depends on these crystal-field components. However, the effect of the mixture within the 7F_2 manifold is estimated to be too small to explain the relation between the transition energy and $\Delta\nu_{\text{hom}}$ of the 5D_0 - 7F_0 line.

Huber⁸ calculated $\Delta\nu_{\text{hom}}$ of the impurity ion in silicate glass due to the two-phonon Raman process in the temperature range of 10–300 K using the distribution of nonacoustic low-frequency phonon modes obtained from inelastic neutron-scattering data. Supposing that the interaction of the optical center with such phonons has the phonon-frequency dependence ($\propto \omega_p^{-1/2}$) typical for the optical phonon, he showed that $\Delta\nu_{\text{hom}}$ has the approximately quadratic temperature dependence down to 40 K and it varies more rapidly at lower temperatures. This result is fairly consistent with the experimental data on the Eu^{3+} -doped glasses,^{3,5,9,11} especially if we consider the contribution from the center-TLS interaction at lower temperatures. If the participation of the nonacoustic low-frequency phonons is dominant, the long-wavelength approximation assumed in the above discussion is not appropriate. It will be reasonable that the interaction of the rare-earth ion with such phonons is expressed in terms of a power series of the amplitude of the lattice vibration instead of the dynamical strain.⁷ If we regard $V^{(n)}$ in the expression (1) as the n th-order expansion coefficient of V with respect to the amplitude a , this revision only leads to the change of the values of X and Y in the above calculations. Therefore, as far as the Eu^{3+} -site dependence of $V_{20}^{(2)}$ and also that of the density of states of phonons to interact with rare-earth ions are negligible, the above discussion holds true for the case of the coupling of the rare-earth ion with nonacoustic phonons.

The homogeneous width of the 5D_0 - 7F_0 transition of the Sm^{2+} ion doped into fluoride glass has a nearly quadratic dependence on temperature in the 30–300 K range.³⁴ Furthermore, at 77 K, $\Delta\nu_{\text{hom}}$ varies approximately linearly with the transition energy and ions with higher transition energies have larger homogeneous widths.³⁷ We previously showed that the 5D_0 - 7F_0 transition energy in this sample is determined by the axial second-order crystal-field parameter B_{20} and that the higher 5D_0 - 7F_0 transition energy corresponds to the larger $|B_{20}|$.⁴³ These properties are the same as those of the 5D_0 - 7F_0 transition of Eu^{3+} in glasses. Thus the above wavelength dependence of $\Delta\nu_{\text{hom}}$ of the 5D_0 - 7F_0 transition of Sm^{2+} in fluoride glass is considered to be explained again by the above mechanism due to the J mixing of 7F_2 into 7F_0 .

B. Dephasing due to the optically active ion-TLS interaction

By transient hole-burning spectroscopy at liquid-He temperature, Schmidt, Macfarlane, and Völker⁶ observed a linear relation between $\Delta\nu_{\text{hom}}$ and the transition energy, which is similar to that observed at room temperature, for the 5D_0 - 7F_0 transition of Eu^{3+} in silicate glass. At such low temperatures, the homogeneous width shows a linear temperature dependence,^{6,11,12} which can be explained by the interaction between the optical center and the TLS.^{9,13–15} In the case of Nd^{3+} -doped glass, the elastic dipole-dipole interaction was estimated to be dominant as the center-TLS interaction compared with the electrostatic multipolar interaction and the direct coupling between the rare-earth ion and the strain field through the spin-orbit interaction.¹⁴ Although the elastic dipole-dipole interaction is different from the electric dipole-dipole interaction, we show that the wavelength dependence of $\Delta\nu_{\text{hom}}$ of the 5D_0 - 7F_0 line of Eu^{3+} in silicate glass at low temperatures can be explained by taking into account the J -mixing effect on the electric dipole-dipole interaction between the center and TLS's. We adopt the spectral diffusion model, in which the spectral line broadens on account of the rapid change in the transition energy of the center caused by the random flip between the metastable states of the TLS. Then $\Delta\nu_{\text{hom}}$ is proportional to the square of the shift in the optical frequency caused by the flip of the TLS. The spectral diffusion was not observed at liquid-He temperature in the temporal range between 10^{-2} and 10^2 s for the 5D_0 - 7F_0 transition of the Eu^{3+} -doped silicate glass.⁶ However, this does not mean the absence of the transition-frequency modulation of a much shorter time scale.

The shift in the optical frequency caused by a flip of the TLS which interact with the optical center through the electric dipole-dipole interaction is proportional to the magnitude of the difference $\Delta\mathbf{P}$ between the permanent electric dipole moment of the center in the excited and ground states. Here we calculate $\Delta\mathbf{P}$ for the 5D_0 - 7F_0 transition of the Eu^{3+} ion. Since the parity of

the wave functions of the 5D_0 and 7F_0 states in the intermediate coupling scheme is a good quantum number, the permanent dipole moments of the Eu^{3+} ion in the 5D_0 and 7F_0 states become zero, when we use the intermediate-coupled wave functions for these two states.

For this reason, we consider the mixing of the opposite-parity high-lying states into the intermediate-coupled 5D_0 and 7F_0 states through the odd-parity component of the crystal-field potential. Then the s component of $\Delta\mathbf{P}$ is written, by using first-order perturbation theory, as

$$\Delta P_s = \sum_{nl\alpha''J''M_{J''}} \{ T_{nl\alpha''J''M_{J''}}^s(4f^6[{}^5D]_0; 4f^6[{}^5D]_0) - T_{nl\alpha''J''M_{J''}}^s(4f^6[{}^7F]_0; 4f^6[{}^7F]_0) \}, \quad (14)$$

with

$$\begin{aligned} & T_{nl\alpha''J''M_{J''}}^s(4f^6[{}^{2S'+1}L']_{JM_{J'}}; 4f^6[{}^{2S+1}L]_{JM_J}) \\ &= - \left[\frac{\langle 4f^6[{}^{2S'+1}L']_{JM_{J'}} | P_s | 4f^5nl\alpha''J''M_{J''} \rangle \langle 4f^5nl\alpha''J''M_{J''} | V^{(0)} | 4f^6[{}^{2S+1}L]_{JM_J} \rangle}{E(nl\alpha''J''M_{J''}) - E([{}^{2S+1}L]_{JM_J})} \right. \\ & \quad \left. + \frac{\langle 4f^6[{}^{2S'+1}L']_{JM_{J'}} | V^{(0)} | 4f^5nl\alpha''J''M_{J''} \rangle \langle 4f^5nl\alpha''J''M_{J''} | P_s | 4f^6[{}^{2S+1}L]_{JM_J} \rangle}{E(nl\alpha''J''M_{J''}) - E([{}^{2S'+1}L']_{JM_{J'}})} \right]. \quad (15) \end{aligned}$$

Here P_s is the s component of the electric dipole moment of the Eu^{3+} ion, and it is expressed as

$$P_s = -e \sum_i r_i C_{1s}(\theta_i, \phi_i),$$

where $-e$ is the electron charge. Further, α represents the additional quantum numbers to define the energy level uniquely. In order to evaluate this expression further, we adopt the closure approximation for the high-lying state $|4f^5nl\alpha''J''M_{J''}\rangle$, which was introduced by Judd⁴⁴ and Ofelt⁴⁵ in order to calculate the oscillator strengths of electric dipole transitions within the $4f$ shell of rare-earth ions. We use the formula

$$\begin{aligned} & Z_{nl}^s(4f^6[{}^{2S'+1}L']_{JM_{J'}}; 4f^6[{}^{2S+1}L]_{JM_J}) \\ & \equiv \sum_{\alpha''J''M_{J''}} T_{nl\alpha''J''M_{J''}}^s(4f^6[{}^{2S'+1}L']_{JM_{J'}}; 4f^6[{}^{2S+1}L]_{JM_J}) \\ & = e \sum_{k,q,\lambda} 14(2\lambda+1)(2l+1)(-1)^{3+s+q+l} B'_{kq} \begin{bmatrix} k & \lambda & 1 \\ q & -s-q & s \end{bmatrix} \begin{bmatrix} 3 & k & l \\ 0 & 0 & 0 \end{bmatrix} \begin{bmatrix} l & 1 & 3 \\ 0 & 0 & 0 \end{bmatrix} \\ & \quad \times \left\{ \begin{matrix} k & \lambda & 1 \\ 3 & l & 3 \end{matrix} \right\} \langle nl|r|4f \rangle \langle 4f^6[{}^{2S'+1}L']_{JM_{J'}} | U_{s+q}^{(\lambda)} | 4f^6[{}^{2S+1}L]_{JM_J} \rangle / \Delta_{lf}, \quad (16) \end{aligned}$$

with

$$\langle nl|r|4f \rangle = \int_0^\infty R(nl)rR(4f)dr,$$

where $R(nl)/r$ and Δ_{lf} are the radial part of the appropriate single nl -electron wave function and the representative energy of $E(nl\alpha''J''M_{J''}) - E([{}^{2S+1}L]_{JM_J})$ and $E(nl\alpha''J''M_{J''}) - E([{}^{2S'+1}L']_{JM_{J'}})$, respectively, and $U_{s+q}^{(\lambda)}$ is the $s+q$ component of the unit tensor operator $\mathbf{U}^{(\lambda)}$ of rank λ . Further, the prime of B'_{kq} represents that the crystal-field parameter values are obtained from the radial integral for the matrix element of $V^{(0)}$ between the $4f^N$ and $4f^{N-1}nl$ states. (It should be noted that, for B_{kq} without the prime, the radial integral is taken for the matrix element between the two $4f^N$ states.) As a result, Eq. (14) is calculated as

$$\Delta P_s \propto \langle 4f^6[{}^5D]_0 | \mathbf{U}^{(0)} | 4f^6[{}^5D]_0 \rangle - \langle 4f^6[{}^7F]_0 | \mathbf{U}^{(0)} | 4f^6[{}^7F]_0 \rangle, \quad (17)$$

and $\Delta\mathbf{P}$ is still estimated to be zero, because $\langle 4f^6[{}^5D]_0 | \mathbf{U}^{(0)} | 4f^6[{}^5D]_0 \rangle$ and $\langle 4f^6[{}^7F]_0 | \mathbf{U}^{(0)} | 4f^6[{}^7F]_0 \rangle$ have the same value. However, the result is revised by the J mixing. We again take into account only the mixing of the 7F_2 state into the 7F_0 state, and neglect the J mixing for 5D_0 for the same reasons that were mentioned in Sec. II A. Then Eq. (14) is calculated as

$$\Delta P_s = \frac{2\sqrt{3}}{15\Delta_{20}} \sum_{q'=-2}^2 \left\{ (-1)^{q'} B_{2q'} \sum_{nl} Z_{nl}^s(4f^6[{}^7F]_0; 4f^6[{}^7F]_{2M_J=q'}) + B_{2-q'} \sum_{nl} Z_{nl}^s(4f^6[{}^7F]_{2M_J=q'}; 4f^6[{}^7F]_0) \right\}. \quad (18)$$

The B_{20} term in this expression is possible to be nonzero when at least one of B_{10} , $B_{1\pm 1}$, B_{30} , and $B_{3\pm 1}$ is present. Some of these crystal-field parameters are present in the point symmetry C_{2v} , C_2 , or C_s of the Eu site. Furthermore, the two summations over nl in the expression (18) are considered to be almost independent of B_{20} in oxide glasses, because the strength of the 5D_0 - 7F_2 transition, which is caused through the same crystal-field terms that are involved in these summations, is almost constant for the variation of B_{20} .^{16,17} Then, if the absolute value of the B_{20} term in expression (18) is sufficiently large compared with those of the other terms, ΔP_e is proportional to B_{20} , and consequently $\Delta\nu_{\text{hom}}$ of the 7F_0 - 5D_0 transition is proportional to B_{20} . Thus the linear relation between $\Delta\nu_{\text{hom}}$ and the transition energy of the 7F_0 - 5D_0 line observed at liquid-He temperature is explained well, provided that the density and properties of the TLS which couple with the Eu^{3+} ion are almost independent of the ion site.

III. CALCULATION OF THE ONE-PHONON 7F_0 - 7F_1 ABSORPTION PROBABILITY

In the Eu^{3+} -doped YAlO_3 crystal, it was shown that the one-phonon absorption from 7F_0 to the lowest-Stark level of 7F_1 is the dominant mechanism of the dephasing of the 7F_0 - 5D_0 transition in the 60–200 K temperature range.⁹ Here we investigate the contribution of the J mixing to the one-phonon 7F_0 - 7F_1 absorption. For simplicity, we assume that the point symmetry of the Eu^{3+}

or Sm^{2+} ion site is not C_1 or S_2 . Since the site symmetry of Eu^{3+} in YAlO_3 crystal is C_s , this restriction is not a problem in comparison with the experiment in this system. Then we can again put $B_{2\pm 1} = 0$, and the wave functions of the Stark levels of 7F_1 are expressed, without the J mixing, as

$$\Psi_1 = |1, 0\rangle, \quad (19a)$$

$$\Psi_2 = \frac{1}{\sqrt{2}}(\theta|1, 1\rangle + |1, -1\rangle), \quad (19b)$$

$$\Psi_3 = \frac{1}{\sqrt{2}}(\theta|1, 1\rangle - |1, -1\rangle), \quad (19c)$$

where $\theta = B_{22}/|B_{22}|$ and $|J, M_J\rangle$ represents the wave function of the M_J component of the 7F_J manifold. On the other hand, the probabilities of the one-phonon 7F_0 - ${}^7F_1(\Psi_j)$ ($j=1, 2, 3$) absorption transitions involve the matrix element $\langle \Psi_j | V^{(1)} | f^6[{}^7F_0] \rangle$. However, when we adopt the wave functions without the J mixing as the 7F_0 and 7F_1 states, this matrix element vanishes because $\langle 4f^6[{}^7F_1]_1 M_J | C_q^{(k)} | 4f^6[{}^7F_0] \rangle$ is zero. Therefore, we take into account the admixture of the 7F_2 state into the 7F_0 and ${}^7F_1(\Psi_j)$ states through the second-order crystal-field potential. We consider only this mixture, because it is the most effective one from the consideration of the magnitude of the energy denominator in the J -mixing coefficient. Then the wave functions of the ${}^7F_1(\Psi_j)$ states are written, by using first-order perturbation theory, as

$$\Psi'_1 = |1, 0\rangle - \frac{\sqrt{3}}{15\Delta_{21}} \{ B_{22}|2, 2\rangle - B_{2-2}|2, -2\rangle \}, \quad (20a)$$

$$\Psi'_2 = \frac{1}{\sqrt{2}} \left\{ (\theta|1, 1\rangle + |1, -1\rangle) + \frac{1}{\Delta_{21}} \left[\frac{1}{10} B_{20}\theta - \frac{\sqrt{6}}{30} B_{22} \right] |2, 1\rangle - \frac{1}{\Delta_{21}} \left[\frac{1}{10} B_{20} - \frac{\sqrt{6}}{30} |B_{22}| \right] |2, -1\rangle \right\}, \quad (20b)$$

$$\Psi'_3 = \frac{1}{\sqrt{2}} \left\{ (\theta|1, 1\rangle - |1, -1\rangle) + \frac{1}{\Delta_{21}} \left[\frac{1}{10} B_{20}\theta + \frac{\sqrt{6}}{30} B_{22} \right] |2, 1\rangle + \frac{1}{\Delta_{21}} \left[\frac{1}{10} B_{20} + \frac{\sqrt{6}}{30} |B_{22}| \right] |2, -1\rangle \right\}. \quad (20c)$$

Using these wave functions and Eq. (7), the matrix element $\langle \Psi'_j | V^{(1)} | 4f^6[{}^7F_0] \rangle$ is calculated as

$$\langle \Psi'_1 | V^{(1)} | 4f^6[{}^7F_0] \rangle = \frac{2}{75} (B_{22} V_{2-2}^{(1)} - B_{22}^* V_{22}^{(1)}) \left(\frac{1}{\Delta_{21}} - \frac{1}{\Delta_{20}} \right), \quad (21a)$$

$$\langle \Psi'_j | V^{(1)} | 4f^6[{}^7F_0] \rangle = \frac{\sqrt{6}}{150} \left[B_{20} \pm \frac{\sqrt{6}}{3} |B_{22}| \right] (V_{21}^{(1)} \theta^* \pm V_{2-1}^{(1)}) \left(\frac{1}{\Delta_{21}} - \frac{1}{\Delta_{20}} \right), \quad (21b)$$

where $j=2, 3$ and θ^* and B_{22}^* are the complex conjugates of θ and B_{22} , respectively. In these equations, the higher-order terms of the second-order crystal-field parameters have been neglected. The minus and plus signs in the right-hand side of Eq. (21b) correspond to the cases of $j=2$ and 3 , respectively. Although the 7F_3 state mixes into 7F_1 by $V_2^{(0)}$, we need not consider this mixture, because $\langle 4f^6[{}^7F_3]_3 M_J | C_{kq} | 4f^6[{}^7F_0] \rangle$ is zero. Equations (21a) and (21b) show that the probabilities of the one-

phonon 7F_0 - ${}^7F_1(\Psi'_j)$ ($j=1, 2, 3$) absorption processes depend largely on the crystal-field parameters on account of the J mixing. For example, it is predicted from Eq. (21a) that the one-phonon 7F_0 - ${}^7F_1(\Psi'_1)$ absorption does not occur in the case of the point symmetries of the rare-earth ion site which require that B_{22} is zero, such as C_n and C_{nv} ($n=3, 4, 6$).

In $\text{YAlO}_3:\text{Eu}^{3+}$, the lowest Stark level of 7F_1 corresponds to Ψ'_2 . The second-order crystal-field parameters

are estimated in this material as $B_{20} = -45 \text{ cm}^{-1}$ and $|B_{22}| = 480 \text{ cm}^{-1}$ from the energy separations of the three 5D_0 - 7F_1 fluorescence lines,⁴⁶ and the quantity in the first parentheses of Eq. (21b), $B_{20} - (\sqrt{6}/3)|B_{22}|$ ($= -437 \text{ cm}^{-1}$), is nonzero. Accordingly, the one-phonon absorption from 7F_0 to the lowest-Stark level of 7F_1 can arise through the second-order crystal-field potential, unless $V_{21}^{(1)}\theta^* = V_{2-1}^{(1)}$.

If we also take into account the dependence of $V^{(n)}$ on the symmetry of the lattice distortion due to phonons, it is predicted from Eq. (21b) that the one-phonon 7F_0 - ${}^7F_1(\Psi'_j)$ ($j=2,3$) absorptions by a phonon of the totally symmetric mode do not occur even through the second-order crystal-field potential except for the point symmetries of C_1 and S_2 , because $V_{2\pm 1}^{(1)}$ for the coupling with a totally symmetric mode are zero from a group-theoretical consideration.

Mitsunaga²⁷ mentioned that the temperature dependence of the stimulated photon echo intensity for the 7F_0 - 5D_0 transition of Eu^{3+} in YAlO_3 below about 20 K may be ascribed to the relaxation between the hyperfine sublevels of the 7F_0 state due to the Orbach process which occurs through the lowest Stark level of the 7F_1 state. The rate of this hyperfine relaxation includes the same matrix elements as that of the one-phonon 7F_0 - 7F_1 absorption process.^{39,40} Accordingly, the contribution of J mixing is essential also for the hyperfine relaxation in the 7F_0 state due to the Orbach process via 7F_1 .

IV. CONCLUDING REMARKS

We have calculated the homogeneous width of the 5D_0 - 7F_0 line of the Eu^{3+} and Sm^{2+} ions in solids. Two-phonon Raman scattering, one-phonon absorption, and the electric dipole-dipole interaction between the rare-earth ion and the flipping TLS have been considered as the dephasing mechanisms. It has been shown that the wave-function mixing through the second-order crystal-field components plays the significant role in the homogeneous broadening of this line due to all the above mechanisms.

It has recently been found by our group^{16,17} that the probability of the optical 5D_0 - 7F_0 transition of the Eu^{3+} ion in various oxide glasses is proportional to the square of the axial second-order crystal-field parameter B_{20} . The interpretation of this result is that the dominant mechanism of the optical 5D_0 - 7F_0 transition of the Eu^{3+} ion in oxide glasses is due to the borrowing of intensity from the 5D_0 - 7F_2 ($M_J=0$) transition by J mixing through $B_{20}C_{20}$. As discussed above, the wavelength dependence

of $\Delta\nu_{\text{hom}}$ of the 5D_0 - 7F_0 transition of Eu^{3+} and Sm^{2+} in glasses can be also accounted for well, by assuming that this J mixing makes the dominant contribution to the rates of the phase relaxation due to the two-phonon Raman process and the electric dipole-dipole interaction between the optical center and the TLS. Moreover, J mixing has been found to be essential in the direct process due to the one-phonon transition between 7F_0 and 7F_1 .

Finally, we make a comment from the viewpoint of the practical application of materials doped with Eu^{3+} and Sm^{2+} ions to wavelength-selective optical memory devices. Many groups have so far made persistent spectral hole-burning measurements for the 5D_0 - 7F_0 transition of these ions in solids.^{22,29-31,33,34} As a result, materials of much interest, such as the Eu^{3+} -doped Y_2SiO_5 crystal³¹ and the Sm^{2+} -doped mixed crystals^{29,30} and glasses,^{33,34} have been found. In the former sample, very many holes are burnable at low temperatures, while, in the latter, hole burning occurs at room temperature. However, a material which satisfies the two requirements of room-temperature operation and sufficiently many holes to be burned has not been found yet. Therefore, further development is necessary. From the consideration of only the 7F_0 - 7F_1 energy separation and the Debye temperature of the host matrices, the one-phonon 7F_0 - 7F_1 absorption is probable to occur at room temperature. This is because the energy separation between 7F_0 and the lowest Stark level of 7F_1 in the Eu^{3+} and Sm^{2+} in solids is roughly equal to the thermal energy at room temperature and also because the Debye temperature of most host material is above this energy separation.^{19,21} As mentioned before, however, the one-phonon 7F_0 - 7F_1 absorption rate can be controlled by the static crystal field acting on the ions or the point symmetry of the ion site. By using Eqs. (21a) and (21b), one may be able to select materials in which the one-phonon 7F_0 - 7F_1 absorption does not participate in the broadening of $\Delta\nu_{\text{hom}}$ of the 7F_0 - 5D_0 transition even at room temperature. Further, if we can find a material in which W_R of Eq. (10) has a very small value because of the cancellation among the terms in $|\cdots|$, the 7F_0 - 5D_0 line of Eu^{3+} and Sm^{2+} is expected to be very narrow even at room temperature.

In conclusion, we emphasize that the static component as well as the dynamic one of the crystal-field potential plays an important role in the phonon-induced relaxations associated with the 5D_0 - 7F_0 transition of Eu^{3+} and Sm^{2+} ions in solids. Our investigation is important because, in addition to its fundamental significance, it provides valuable information in choosing useful materials for optical memory devices.

¹For a review, see J. Lumin. **36** (1987).

²T. Kushida and E. Takushi (unpublished).

³P. Avouris, A. Campion, and M. A. El-Sayed, J. Chem. Phys. **67**, 3397 (1977).

⁴J. R. Morgan, E. P. Chock, W. D. Hopewell, M. A. El-Sayed, and R. Orbach, J. Phys. Chem. **85**, 747 (1981).

⁵G. S. Dixon, R. C. Powell, and X. Gang, Phys. Rev. B **33**, 2713 (1986); F. Durville, G. S. Dixon, and R. C. Powell, J. Lumin.

36, 221 (1987). In these references, it has been shown that the homogeneous width of the 5D_0 - 7F_0 transition of the Eu^{3+} ion in lithium silicate glass is exceptionally smaller on the higher-energy side of the inhomogeneously broadened profile of this transition between about 50 and 200 K. This is the opposite property to the homogeneous width of the many other Eu^{3+} -doped oxide glasses. We will not discuss this result for the lithium silicate glass host in the present paper.

- ⁶Th. Schmidt, R. M. Macfarlane, and S. Völker, *Phys. Rev. B* **50**, 15 707 (1994).
- ⁷D. L. Huber, *J. Non-Cryst. Solids* **51**, 241 (1982).
- ⁸D. L. Huber, *J. Lumin.* **36**, 327 (1987).
- ⁹P. M. Selzer, D. L. Huber, D. S. Hamilton, W. M. Yen, and M. J. Weber, *Phys. Rev. Lett.* **36**, 813 (1976).
- ¹⁰J. R. Morgan and M. A. El-Sayed, *Chem. Phys. Lett.* **84**, 213 (1981).
- ¹¹R. Yano, M. Mitsunaga, N. Uesugi, and M. Shimizu, *Phys. Rev. B* **50**, 9031 (1994).
- ¹²Th. Schmidt, J. Baak, D. A. van de Straat, H. B. Brom, and S. Völker, *Phys. Rev. Lett.* **71**, 3031 (1993).
- ¹³S. K. Lyo, *Phys. Rev. Lett.* **48**, 688 (1982).
- ¹⁴D. L. Huber, M. M. Broer, and B. Golding, *Phys. Rev. Lett.* **52**, 2281 (1984).
- ¹⁵D. L. Huber, *J. Lumin.* **36**, 307 (1987).
- ¹⁶G. Nishimura and T. Kushida, *Phys. Rev. B* **37**, 9075 (1988); *J. Phys. Soc. Jpn.* **60**, 683 (1991); **60**, 695 (1991).
- ¹⁷M. Tanaka, G. Nishimura, and T. Kushida, *Phys. Rev. B* **49**, 16917 (1994). There are three typographical errors in Eq. (8) in this reference. The correct equation should be read
- $$\langle [f^6 {}^7F_0] | \mu | [f^6 {}^5D_0] \rangle$$
- $$= T({}^5D_0 \rightarrow {}^7F_0) - \frac{2\sqrt{3}}{15\Delta_{20}} \sum_{q=-2}^2 (-1)^q B_{2q}^* T({}^5D_0 \rightarrow {}^7F_2 M_J = q).$$
- Here, B_{2q}^* is the complex conjugate of B_{2q} .
- ¹⁸W. M. Yen, W. C. Scott, and A. L. Schawlow, *Phys. Rev.* **136**, A271 (1964).
- ¹⁹T. Kushida, *Phys. Rev.* **185**, 500 (1969).
- ²⁰P. Hill and S. Hufner, *Z. Phys.* **240**, 168 (1970).
- ²¹J. M. Pellegrino and W. M. Yen, *Phys. Rev. B* **24**, 6719 (1981).
- ²²A. Winnacker, R. M. Shelby, and R. M. Macfarlane, *Opt. Lett.* **10**, 350 (1985).
- ²³R. M. Macfarlane and R. M. Shelby, in *Spectroscopy of Solids Containing Rare Earth Ions*, edited by A. A. Kaplyanskii and R. M. Macfarlane (North-Holland, Amsterdam, 1987), p. 51.
- ²⁴R. van den Berg and S. Völker, *Chem. Phys. Lett.* **150**, 491 (1988).
- ²⁵W. R. Babbitt, A. Lezama, and T. W. Mossberg, *Phys. Rev. B* **39**, 1987 (1989).
- ²⁶M. Mitsunaga and N. Uesugi, *Opt. Lett.* **15**, 195 (1990).
- ²⁷M. Mitsunaga, *Phys. Rev. A* **42**, 1617 (1990).
- ²⁸J. Ganem, Y. P. Wang, D. Boye, R. S. Meltzer, W. M. Yen, and R. M. Macfarlane, *Phys. Rev. Lett.* **66**, 695 (1991).
- ²⁹R. Jaaniso and H. Bill, *Europhys. Lett.* **16**, 569 (1991).
- ³⁰K. Holliday, C. Wei, M. Croci, and U. S. Wild, *J. Lumin.* **53**, 227 (1992).
- ³¹R. Yano, M. Mitsunaga, and N. Uesugi, *Opt. Lett.* **16**, 1884 (1991).
- ³²R. Yano, M. Mitsunaga, and N. Uesugi, *Phys. Rev. B* **45**, 12 752 (1992); M. Mitsunaga, R. Yano, and N. Uesugi, *ibid.* **45**, 12 760 (1992).
- ³³K. Hirao, S. Todoroki, D. H. Cho, and N. Soga, *Opt. Lett.* **18**, 1586 (1993).
- ³⁴A. Kurita, T. Kushida, T. Izumitani, and M. Matsukawa, *Opt. Lett.* **19**, 314 (1994).
- ³⁵G. P. Flinn, K. W. Jang, J. Ganem, M. L. Jones, R. S. Meltzer, and R. M. Macfarlane, *Phys. Rev. B* **49**, 5821 (1994).
- ³⁶R. W. Equall, Y. Sun, R. L. Cone, and R. M. Macfarlane, *Phys. Rev. Lett.* **72**, 2179 (1994).
- ³⁷A. Kurita, M. Tanaka, T. Hiyama, A. Hada, and T. Kushida, *J. Lumin.* (to be published).
- ³⁸G. S. Ofelt, *J. Chem. Phys.* **38**, 2171 (1963).
- ³⁹B. Henderson and G. F. Imbusch, *Optical Spectroscopy of Inorganic Solids* (Clarendon, Oxford, 1989), p. 183.
- ⁴⁰R. Orbach, *Proc. Roy. Soc. (London) A* **264**, 458 (1961).
- ⁴¹R. Orbach, *Phys. Rev.* **133**, A34 (1964).
- ⁴²C. Brecher and L. A. Riseberg, *Phys. Rev. B* **13**, 81 (1976).
- ⁴³M. Tanaka and T. Kushida, *Phys. Rev. B* **49**, 5192 (1994).
- ⁴⁴B. R. Judd, *Phys. Rev.* **127**, 750 (1962).
- ⁴⁵G. S. Ofelt, *J. Chem. Phys.* **37**, 511 (1962).
- ⁴⁶L. E. Erickson and K. K. Sharma, *Phys. Rev. B* **24**, 3697 (1981).